ADVANCED FUNCTIONAL MATERIALS
www.afm-journal.de

Antibiotic-Releasing Silk Biomaterials for Infection Prevention and Treatment

*Eleanor M. Pritchard, Thomas Valentin, Bruce Panilaitis, Fiorenzo Omenetto, and David L. Kaplan**

Effective treatment of infections in avascular and necrotic tissues can be challenging due to limited penetration into the target tissue and systemic toxicities. Controlled-release polymer implants have the potential to achieve the high local concentrations needed while also minimizing systemic exposure. Silk biomaterials possess unique characteristics for antibiotic delivery, including biocompatibility, tunable biodegradation, stabilizing effects, water-based processing, and diverse material formats. The functional release of antibiotics spanning a range of chemical properties from different material formats of silk (films, microspheres, hydrogels, coatings) is reported. The release of penicillin and ampicillin from bulk-loaded silk films, drug-loaded silk microspheres suspended in silk hydrogels and bulk-loaded silk hydrogels is investigated and the in vivo efficacy of the ampicillin-releasing silk hydrogels is demonstrated in a murine infected-wound model. Silk sponges with nanofilm coatings are loaded with gentamicin and cefazolin, and release is sustained for 5 and 3 days, respectively. The capability of silk antibiotic carriers to sequester, stabilize, and then release bioactive antibiotics represents a major advantage over implants and pumps based on liquid drug reservoirs, where instability at room or body temperature is limiting. The present studies demonstrate that silk biomaterials represent a novel, customizable antibiotic platform for focal delivery of antibiotics using a range of material formats (injectable to implantable).

Antibiotics are an essential component of infection treatment and prevention. In cases where systemic drug penetration into ischemic, avascular and necrotic tissues is limited (including treatment of abscesses,[1–3] bone infections,[4] and post-operative tissue), controlled-release polymers have the potential to reduce side effects and increase efficacy by releasing antibiotics locally at a target site of interest.[5–8] Toward this goal, various biodegradable polymeric biomaterials have been explored for antibiotic delivery, including synthetic polymers like poly(lactide-*co*-glycolide) and polycaprolactone, and natural polymers like collagen and chitosan. However, these polymer systems suffer from a number of drawbacks including harsh processing conditions or poor biocompatibility in the case of the synthetic polymers, and rapid degradation and poor tunability for the natural polymers.[9–11]

Silk fibroin is a biologically derived protein polymer purified from domesticated silkworm (*Bombyx mori*) cocoons and has demonstrated excellent properties for drug delivery, including biocompatibility,[12–16] robust mechanical strength in various materials formats,[17] and controllable rates of biodegradation to nontoxic products in vivo.[18] The degradation time course of silk implants can be controlled from days to years via regulation of the β-sheet content (crystallinity).[19,20] Silk can be processed entirely in aqueous systems using mild, ambient conditions of temperature and pressure, allowing the incorporation of sensitive compounds and proteins without loss of bioactivity.[21,22]

A variety of silk fibroin biomaterials have been explored for sustained small-molecule delivery, including porous sponges, films and coatings, hydrogels, and micro- and nanoparticles.[20,23,24] The release behavior of these compounds from silk carriers is tunable, based on the manipulation of multiple control points during the process of preparing the silk polymer, including carrier morphology, molecular weight, and crystallinity/β-sheet content.[23,24] The combined diversity of material formats for drug delivery, tight control of the drug-carrier features, and the unique combination of properties of the silk material (biocompatibility, biodegradation, aqueous processing) result in a broad range of silk-based delivery systems for focal antibiotic delivery. Furthermore, silk films exert a remarkable stabilizing effect on encapsulated enzymes[25,26] and antibodies,[27] suggesting improved antibiotic stability derived from encapsulation in silk as another critical benefit in using this protein material system.

The objective of the present study was to demonstrate the utility of silk-based biomaterials to address the need for focal antibiotic delivery by investigating the loading and release of a variety of antibiotics in different silk material formats. Antibiotic release from silk biomaterials was evaluated based on the inhibition of Gram negative *Escherichia coli* (*E. coli*) ATCC 25922 and gram positive *Staphylococcus aureus* (*S. aureus*) ATCC 25923, pathogens that are frequently isolated from surgical site infections. The silk material formats studied included bulk-loaded

Dr. E. M. Pritchard, T. Valentin, Prof. B. Panilaitis, Prof. F. Omenetto, Prof D. L. Kaplan
Department for Biomedical Engineering
Tufts University
Medford, MA 02155, USA
E-mail: david.kaplan@tufts.edu

DOI: 10.1002/adfm.201201636

Table 1. Ampicillin film release: high loading = 2 mg mL^{-1} ampicillin in a 6% (w/v) silk solution (theoretical load = 0.4 mg per film); low loading = 1 mg mL^{-1} ampicillin in a 6% (w/v) silk solution (theoretical load = 0.2 mg per film).

	High Loading/Methanol treated	High Loading/Untreated	Low Loading/Methanol treated	Low Loading/Untreated
Average ampicillin release [μg]	213.84 ± 50.52	176.14 ± 45.49	68.47 ± 9.25	68.33 ± 22.96
Fraction of total theoretical film load released in the first 24 h	0.53	0.44	0.34	0.34

Table 2. Penicillin film release: high loading = 4 mg mL^{-1} penicillin in a 6% (w/v) silk solution (theoretical load = 0.8 mg per film); low loading = 1 mg mL^{-1} penicillin in a 6% (w/v) silk solution (theoretical load = 0.4 mg per film).

	High Loading/Methanol treated	High Loading/Untreated	Low Loading/Methanol treated	Low Loading/Untreated
Average penicillin release [μg]	345.87 ± 140.94	167.08 ± 24.82	193.98 ± 5.03	205.88 ± 22.58
Fraction of total theoretical film load released in the first 24 h	0.43	0.21	0.48	0.51

silk films, 3D porous sponges, nanofilm coatings, bulk and microsphere-loaded hydrogels and degummed silk fibers.

Implants are most susceptible to surface bacterial colonization during a 6 h post-implantation "decisive period,"[8] making the first 24 h of antibiotic release most critical in the prevention of bacterial adhesion and long-term implant success. The first 24 h of bacterial inhibition capability were evaluated for silk films loaded with varied concentrations of ampicillin and penicillin (0.4 mg per film and 0.2 mg per film for ampicillin-loaded films and 0.8 mg per film and 0.4 mg per film for penicillin-loaded films) which were either treated with methanol for 5 min or left untreated. No reduction in activity was seen in the methanol treated films compared with the untreated films (**Table 1**,**2**), suggesting that methanol treatment did not degrade the incorporated antibiotic. The films delivered approximately half of their initial load of ampicillin within the first 24 h of bacterial exposure. The fraction of the total load recovered was lower in the untreated highly loaded films than in the methanol-treated films, possibly because bioactivity was lost when the film was resolubilized on the agar lawn (as opposed to eluting slowly from insoluble methanol-treated films) (Table 1,2).

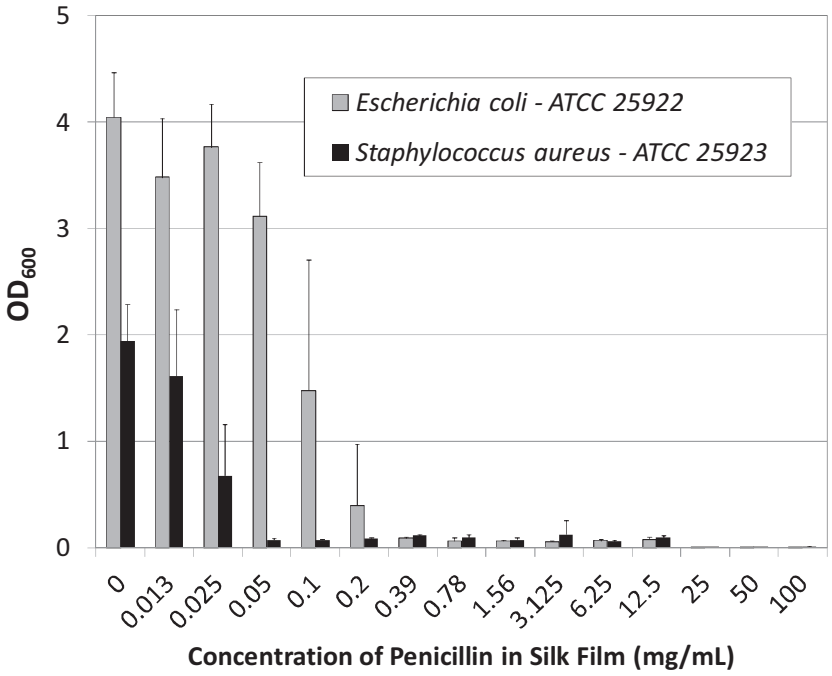

Figure 1. Antibiotic release from bulk-loaded silk films: optical density of *S. aureus* and *E. coli* liquid cultures at 600 nm (OD_{600}) after 24 h incubation at 37 °C relative to the concentration of penicillin used in the preparation of antibiotic silk films. $N = 3$. The error bars represent the standard deviations.

To determine the minimum inhibitory penicillin-loading concentration in silk films, silk solutions loaded with varied penicillin concentrations (100 mg mL^{-1} to 0.013 mg mL^{-1}) were cast into films and exposed to liquid cultures of *E. coli* and *S. aureus*. For both bacteria, complete inhibition was found in liquid cultures exposed to the films prepared with 25, 50, or 100 mg or penicillin per mL of silk (5, 10, and 20 mg of penicillin per film, respectively) (**Figure 1**). The 0.39 mg mL^{-1} and 0.05 mg mL^{-1} concentrations reduced the optical density at 600 nm, OD_{600}, of the liquid cultures to less than 5% of the control culture OD_{600} in *E. coli* and *S. aureus*, respectively (Figure 1). These results suggest that, when prepared with sufficient drug concentrations, silk films can be used to prevent infection and suppress bacterial growth totally. Silk-film coatings can achieve high local concentrations that cannot be administered systemically due to side-effects, as mentioned earlier.

Layer-by-layer nanofilm coatings were studied as a potential strategy for functionalizing porous 3D substrates with water-soluble antibiotics. The release duration was 5 d for gentamicin-loaded sponges and 3 d for cefazolin-loaded sponges (**Figure 2**). For the gentamicin-loaded scaffolds, the total loading was 107.5 ± 31.0 μg ($n = 4$ samples) and for the cefazolin-loaded scaffolds, the total loading was 55.5 ± 7.0 μg ($n = 3$ samples). The gentamicin-loaded scaffolds released approximately 40 μg

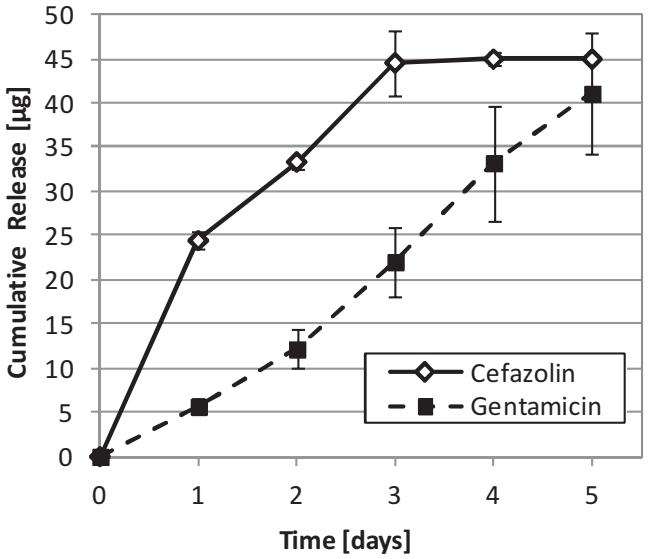

Figure 2. Antibiotic release from silk-nanofilm coatings on silk sponges. Cumulative release of gentamicin and cefazolin from nanofilm-coated porous silk sponges on *S. aureus* lawns. $N = 3$. The error bars represent the standard deviation.

over 5 d and the cefazolin-loaded scaffolds released approximately 45 µg over 3 d (Figure 2). Gentimicin release from sponges, determined based on the clearance of both *S. aureus* and *E. coli*, shows good agreement (Supporting Information, Figure S1). This suggests that nanofilm coatings can be used to achieve constant, sustained release of water-soluble drugs from porous sponge substrates. Both the silk-nanofilm layer-by-layer coating process and macroscale, bulk-loaded silk films could be useful for building antibiotic release into medical materials with conformal coatings that would benefit from microbial resistance, such as bandages, porous sponge packing materials, tissue-engineering scaffolds, and implants. Proof-of-concept data on an example application is shown in Figure S2 in the Supporting Information. We have previously described the ability to control the release behavior from silk-film and nanofilm coatings through manipulation of the morphology and silk material properties,[28,29] amplifying the utility of the silk delivery systems to control infection.

Systems for injectable delivery (bulk-loaded silk hydrogels and silk gels loaded with drug-releasing silk microspheres) were evaluated in vitro and in vivo. Sonication of silk induces the sol-gel transition of the silk solution to stable, β-sheet rich, physically crosslinked networks without requiring chemical agents.[30] Sonication-induced silk hydrogels are also characterized by a highly tunable gelation behavior: the conditions of hydrogel formation can be precisely controlled to ensure the silk solution remains in the liquid state long enough post-sonication to mix in other components, such as cells, microspheres, or antibiotic suspensions, and injected to complete the transition to a physically crosslinked hydrogel in vivo. The total loading of the microspheres was approximately 0.5 mg of antibiotic per mg of microspheres (encapsulation efficiency (determined as previously described)[31] of approximately 80%). In vitro (zone of inhibition (ZOI) in *S. aureus* lawns) bulk-loaded gels exhausted their penicillin load within 48 h and ampicillin within 72 h (**Figure 3**A,B). The concentration of the silk hydrogel (4% (w/v) compared with 8% (w/v)) did not impact on the penicillin release behavior (Supporting Information, Figure S3). Microsphere-loaded gels released at a lower daily release rate than bulk-loaded systems, but exhibited longer release durations (4 d). These two different loading strategies provide different release profiles; rapid release from bulk-loaded hydrogels compared with slower, more-sustained release from microspheres

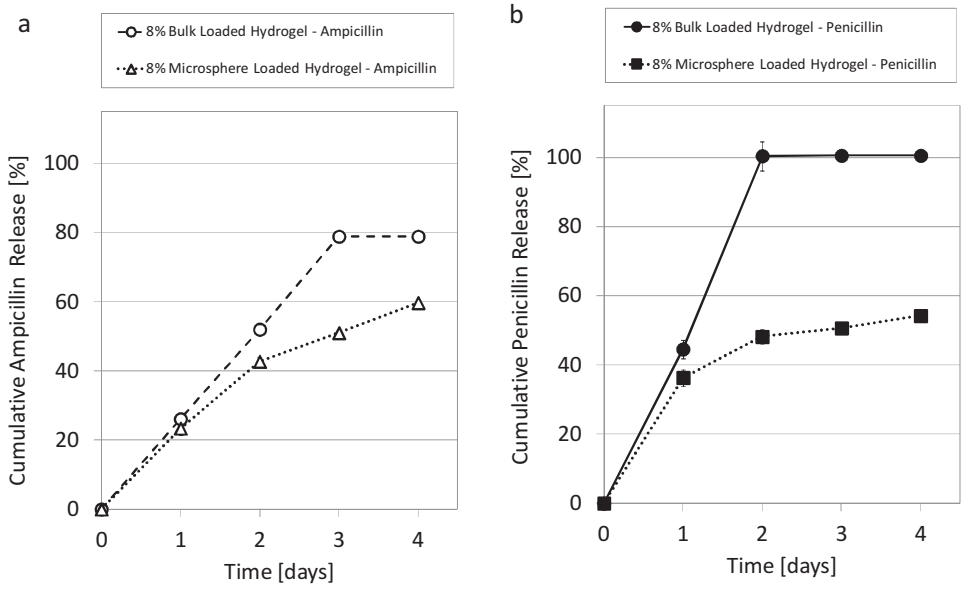

Figure 3. In vitro testing of antibiotic-releasing silk hydrogels. A,B) Cumulative drug release from penicillin-loaded (a) and ampicillin-loaded (b) silk gels. The gels were prepared either by mixing penicillin or ampicillin into the silk solution post-sonication/pre-gelation (bulk loaded) or by mixing antibiotic-loaded silk microspheres into the silk solution post-sonication/pre-gelation (microsphere loaded). $N = 3$. The error bars represent standard deviations. Where error bars are not shown, they fall into background.

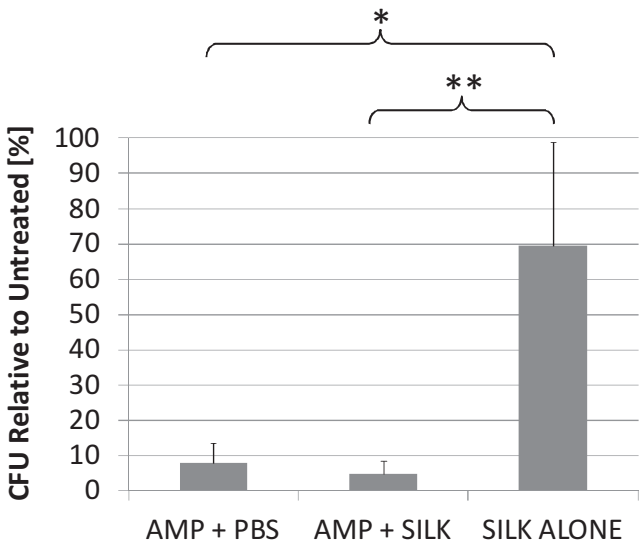

Figure 4. In vivo testing of antibiotic-releasing silk hydrogels. The total *S. aureus* CFU counts for various wound treatments relative to the total *S. aureus* CFU for untreated wounds are shown, with the following treatment groups: AMP + PBS (250 μg mL^{-1} mL^{-1} ampicillin in sterile phosphate buffered saline (PBS)), AMP + SILK (250 μg mL^{-1} ampicillin bulk loaded into 4% (w/v) silk hydrogel) and SILK ALONE (unloaded 4% (w/v) silk hydrogel). $N = 5$. The error bars represent the standard deviations. The data were analyzed using a two-tailed *t*-test, $df = 8$; the significance levels of the individual tests are indicated: *: $P < 0.05$, **: $P < 0.01$.

suspended in hydrogels. These two injectable delivery formats can be combined to achieve the desired combination of physical properties and release kinetics.

The in vivo efficacy of bulk-loaded ampicillin-releasing silk hydrogels was evaluated in an infected murine wound model. *S. aureus*-infected wounds treated with injections of ampicillin-releasing silk hydrogels were compared with wounds treated with injections of ampicillin in aqueous solution: both wounds which received injections of unloaded silk hydrogel and untreated wounds. For comparison, the colony forming unit (CFU) count for each treatment was divided by the CFU count for the untreated wound (**Figure 4**) (individual animal results without normalization are reported in Supporting Information, Table S1). Wounds treated with ampicillin in solution (AMP + PBS) had CFU counts that averaged 8.1 ± 5.7% of the untreated-wound CFU counts. Wounds treated with ampicillin-releasing silk hydrogels (AMP + SILK) had CFU counts that averaged 4.8 ± 3.7% of the untreated-wound CFU counts, approximately a 20-fold reduction. Wounds receiving unloaded silk hydrogels (SILK ALONE) had CFU counts that averaged 69.5 ± 29.5% of the untreated-wound CFU counts. The difference in average CFU count in wounds treated with ampicillin-releasing silk hydrogel and wounds receiving unloaded silk hydrogel (two-tailed *t*-test, $df = 8$, $p < 0.01$).

The reduction in the average CFU count for wounds treated with ampicillin-releasing silk hydrogel compared with that arising from a local injection of ampicillin in PBS was not statistically significant, but this is an expected result given that the wounds were analyzed 24 h after treatment (longer durations were not investigated due to the presence of untreated control infections on every mouse). Over a short time frame, the therapeutic benefit of sustained release and/or the presence of filler material might not be detectable; in vitro data suggested the bulk-loaded silk hydrogels sustained ampicillin release up to 3 d and continued to suppress bacterial growth during that time frame, while the ampicillin in PBS was expected to dissipate rapidly, allowing the bacterial population that survived the initial exposure to repopulate the wound site. Future work will include longer therapeutic time frames, but the preliminary study demonstrated the feasibility of silk hydrogels for injectable antibiotic delivery. In addition, the observation that the total CFU counts for wounds receiving ampicillin injections (either in PBS or silk hydrogel) were reduced compared with the untreated wounds and wounds injected with unloaded silk hydrogel suggests that the antibacterial effect is localized.

Antibiotics with low water solubility are difficult to administer using conventional methods because the high systemic doses required cannot be prepared in aqueous solutions. To test the loading and delivery of antibiotics with a high methanol solubility and low water solubility from silk biomaterials, rifampicin ($\log P = 2.7$, aqueous solubility = 2.5 mg mL^{-1}) and erythromycin ($\log P = 1.2$, aqueous solubility = 2.0 mg mL^{-1}) were chosen for study. To deliver hydrophobic, alcohol soluble drugs from silk biomaterials a high-concentration solution of the compound of interest was prepared in methanol, then the silk biomaterial substrate was immersed in the drug-saturated methanol. During the methanol soaking, the compound was able to move into the polymer network of the silk until equilibrium was achieved. Once the drug-loaded biomaterial was immersed in an aqueous solution, diffusion of the "trapped" drug out of the silk carrier was limited by the drug's solubility in water. As a result, slow, sustained, constant release was achieved. **Figure 5**A shows a rifampicin-loaded silk fiber after soaking and drying. Figure 5B,C show zones of clearance in

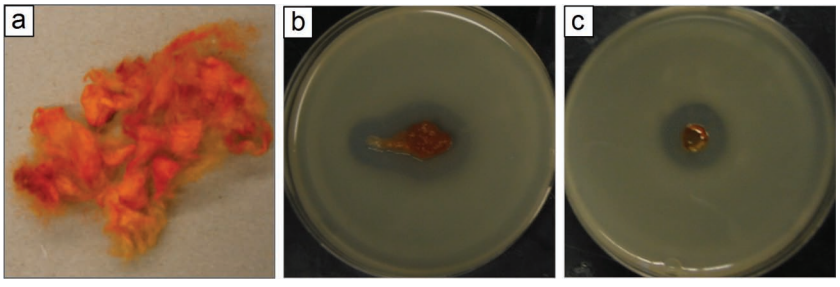

Figure 5. Bacterial lawn growth inhibition induced by rifampicin-releasing silk biomaterials. A) Silk fibers after immersion in a 20 mg mL^{-1} solution of rifampicin in methanol overnight, rinsing in distilled water, and drying. B) Representative sample agar plate showing the zone of inhibition in an *S. aureus* lawn produced by rifampicin-releasing silk fibers. C) Representative sample agar plate showing the zones of inhibition in an *S. aureus* lawn produced by rifampicin-releasing silk film.

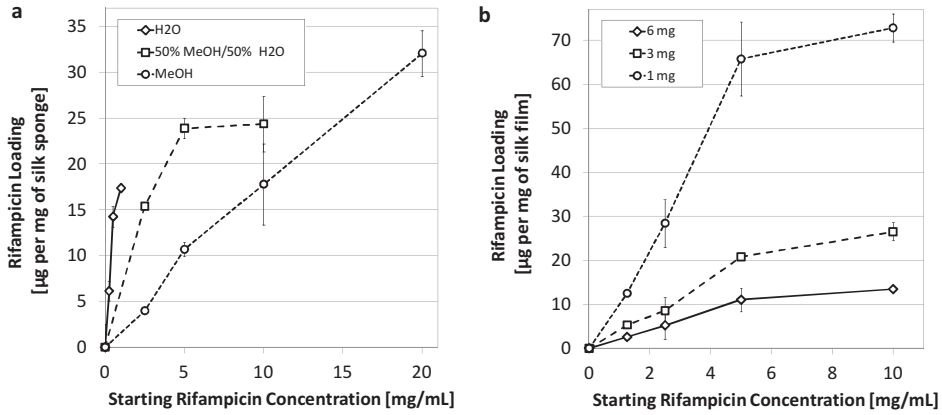

Figure 6. Rifampicin loading in silk biomaterials. A) Rifampicin loading in silk sponges versus starting rifampicin soaking solution concentration for varied soaking solution solvents B) Rifampicin loading in silk films versus starting rifampicin concentration in the methanol soak solution for varied film thickness (in mg of silk film).

S. aureus lawns produced by a rifampicin-loaded silk fiber and silk film, respectively. Plots of rifampicin loading versus concentration in the soak solution for silk sponges and silk films are shown in **Figure 6**A and Figure 6B, respectively.

The rifampicin-loaded sponges exhibited a release duration of 8–9 days (**Figure 7**B) while films exhibited burst release; >85% of the cumulative release was released within the first 24 h for films (Figure 7A). Good agreement was observed between the cumulative-release curves generated using ZOI data and the UV-absorbance data, suggesting the drug activity was preserved during loading and the duration of the release study (Figure 7A,B). Rifampicin release from films was faster than from sponges or fibers, likely due to the short path length and the difference in material diffusivity. Rifampicin-loaded silk fibers produced zones of clearance in *S. aureus* lawns for 8 days (Supporting Information, Figure S4).

Longer release durations from silk biomaterials can be achieved through selection of the chemical properties of the antibiotic, as we demonstrate with silk sponges loaded with erythromycin (more soluble in alcohol than rifampicin, and less soluble in water). Erythromycin was loaded into porous silk sponges soaked for 24 hours in solutions of erythromycin in methanol (5 mg mL^{-1}, 50 mg mL^{-1}, and 500 mg mL^{-1}). Release was sustained for at least two weeks from the scaffolds prepared from the 50 mg mL^{-1} solution (**Figure 8**A). At the highest erythromycin loading (500 mg mL^{-1} initial methanol soak solution), continuous release was sustained for at least 31 d (Figure 8B). The release rate did not scale linearly with preliminary erythromycin concentration, likely due to drug release being limited by the solubility of erythromycin in water. However, loading did impact the release behavior and some amount of early burst release was observed. This suggests that the drug concentration in the methanol soaking solution can affect the diffusion gradient and thereby manipulate the release behavior, though maxima are anticipated, where increased loading would have no further effect on release rate due to low compound water solubility. Different material formats (films vs. porous sponges) and initial drug concentrations in the methanol soaking solution produced different release behaviors, which suggests that silk drug carriers can be customized to suit specific applications, including rapid burst release (>85% within the first 24 h) and sustained, long-term release (up to 31 d).

An effective sustained-release drug carrier must preserve the bioactivity of the incorporated therapeutic during fabrication,

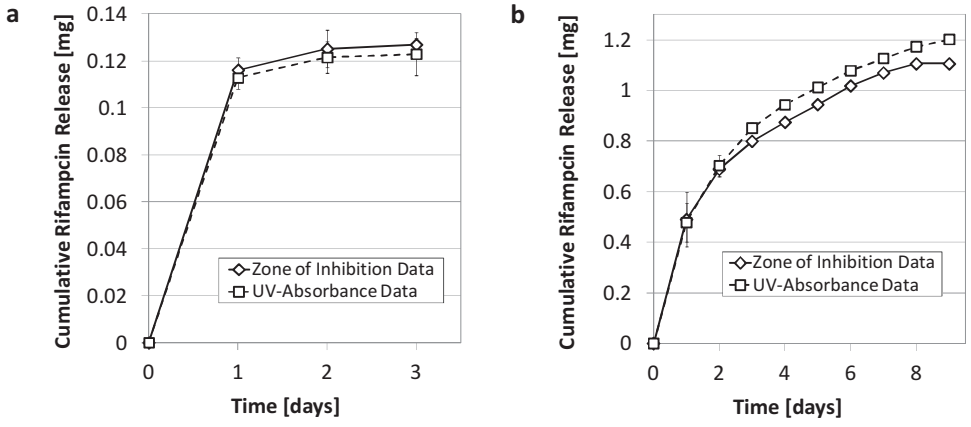

Figure 7. Rifampicin release from silk biomaterials. A,B) Cumulative rifampicin release from silk films (A) and silk sponges (B). $N = 3$. The error bars represent standard deviations; where error bars are not shown, they fall into background.

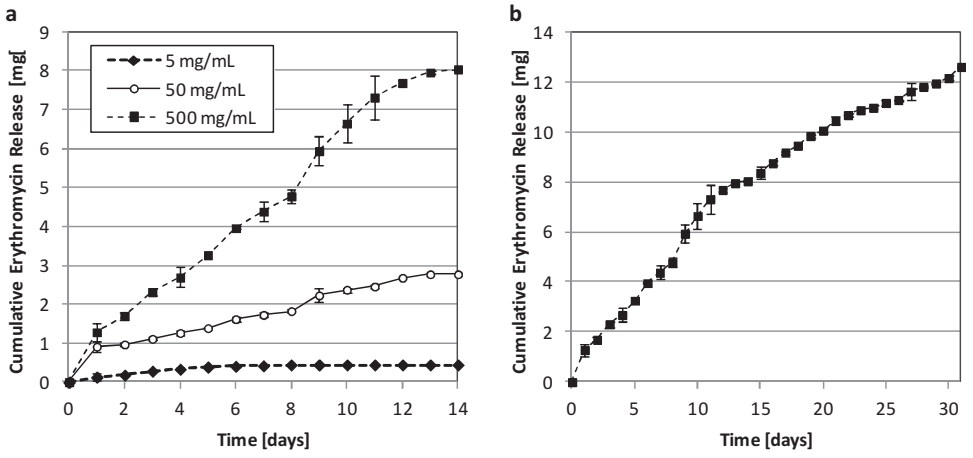

Figure 8. Erythromycin release from silk biomaterials. A) Cumulative erythromycin release over 14 d from porous silk sponges loaded by soaking in 5 mg mL^{-1}, 50 mg mL^{-1}, and 500 mg mL^{-1} solutions of erythromycin in methanol. B) Release from sponges prepared using the highest loading concentration (500 mg mL^{-1}) over 31 d. $N = 3$. The error bars represent the standard deviations.

storage and delivery in vivo. As silk can be processed using mild, aqueous processing at ambient conditions, the bioactivity of sensitive therapeutics is preserved during fabrication.[21,22] We found no loss of ampicillin or penicillin activity following the physical crosslinking of the silk films (Table 1,2). Good agreement was observed between release data based on the clearance zone and the UV-absorbance for the rifampicin-releasing films and sponges (Figure 7A,B), further suggesting that antibiotic bioactivity is preserved during carrier fabrication. In addition to the stabilization of compounds stored in the dry silk films that we have reported previously,[22,25,26] here we show silk is also capable of exerting dramatic stabilization effects in more-challenging conditions: erythromycin is highly unstable in aqueous media,[32] but despite being incubated at 37 °C for over a month in a hydrated silk sponge, erythromycin continued to inhibit *S. aureus* growth for 31d (Figure 8B).

Effective, controllable loading and the release of a range of antibiotics (penicillin, ampicillin, gentamicin, cefazolin, rifampicin, and erythromycin) was demonstrated in a variety of silk biomaterials, including fibers, sponges, nanofilm coatings, films, microspheres, and hydrogels. The range of loading strategies, material properties, release behavior, and antibiotics represented here could be applied to a variety of prophylactic and curative antibiotic therapies. In addition to adding antibiotic-eluting silk coatings to implants (including bone implants and vascular grafts) to prevent infection and biofilm formation, antibiotic-releasing silk biomaterials could be applied at the site of implant removal to aid in wound healing (particularly the highly conformal[33] and injectable, space-filling[34] silk platforms recently described). Silk fibrous materials could be loaded with antibiotics for functionalized sutures, reinforcement meshes, bandages, and gauze. Injectable delivery systems can provide minimally invasive local delivery and be used as degradable abscess filler materials to prevent collapse following drainage. As silk has been extensively investigated as a tissue-engineering scaffold material,[35] we anticipate these antibiotic delivery strategies could also be interfaced with tissue engineering and regenerative medicine approaches to further improve wound-healing outcomes. When the data presented here are combined with the remarkable mechanical features and dramatic stabilization effects of silk materials, a robust stabilization and delivery platform can be envisaged based on this approach, extending into even convenient microneedle formats.[36]

The unique properties of silk, including biocompatibility, tunable biodegradation rate, stabilizing effects, water-based processing, and diverse material formats make it well suited to antibiotic delivery. The present studies provide data to demonstrate that antibiotics can be controllably released from silk biomaterials to repress local bacteria growth. Multiple loading approaches are demonstrated for a broad range of silk material formats, including bulk loading, microsphere embedding, methanol-assisted impregnation, and nanofilm coating. We anticipate the variety of material formats, release profiles and antibiotics described will have broad applicability in focal antibiotic delivery for the treatment of infections that are currently difficult to prevent or cure with conventional systemic delivery alone.

Experimental Section

Materials: The bacteria strains used were *E. coli* ATCC 25922 and *S. aureus* ATCC 25923 (American Type Culture Collection, Manassas, VA). Antibiotics (penicillin G sodium salt, ampicillin sodium salt, cefazolin, gentamicin, rifampicin, erythromycin, and tetracycline) were purchased from Sigma–Aldrich (St. Louis, MO). Bacterial culture dishes, BD-brand Luria–Bertani broth, Miller (formula per liter = 10 g tryptone, 5 g yeast extract, 10 g sodium chloride), BD-brand Luria–Bertani agar, Miller (formula per liter = 10 g tryptone, 5 g yeast extract, 10 g sodium chloride, 15 g agar), Tryptic Soy broth (formula per liter = 17 g pancreatic digest of casein, 3 g papaic digest of soybean, 2.5 g dextrose, 5 g sodium chloride, 2.5 g dipotassium phosphate) and Tryptic Soy agar (formula per liter = 15 g pancreatic digest of casein, 5 g papaic digest of soybean, 5 g sodium chloride, 15 g agar) were purchased from Fisher Scientific (Pittsburgh, PA).

Silk-Solution and Materials Preparation: Silk-fibroin solution was prepared from *B. mori* cocoons as we have described previously.[37] Briefly, cocoons were boiled for either 30 min or 60 min in a solution of Na_2CO_3 (0.02 M) and rinsed, then dried at ambient conditions overnight. The dried fibroin was solubilized in a aqueous LiBr (9.3 M) solution at 60 °C for 2–4 h, yielding a 20% (w/v) solution. LiBr was then

removed from the silk by dialyzing the solution against distilled water for 2.5 d using Slide-a-Lyzer dialysis cassettes (molecular-weight cutoff (MWCO) = 3500 g mol^{-1}, Pierce Thermo Scientific Inc., Rockford, IL). The silk-fibroin concentration was determined by evaporating water from a solution sample of known volume and weighing using an analytical balance. The silk solutions were stored at 4–7 °C before use.

Bulk antibiotic-loaded silk films were prepared as previously described.[28] Microspheres were prepared according to the phospholipid template protocol previously described.[31]

Water-based porous scaffolds were prepared as we have previously described.[38] Nanofilm coatings were applied using our previously described protocol,[29] modified to accommodate the coating of a 3D porous scaffold.[39] Silk hydrogels were prepared using sonication-induced gelation as we have previously described.[30] For additional details on fabrication of antibiotic-loaded silk films, silk microspheres, water-based porous scaffolds, silk nanofilm coatings, and silk hydrogels, see Supporting Information.

Bacteria Culture: Luria–Bertani (LB) and Tryptic Soy Broth were prepared according to the manufacturer's instructions and aliquots were made up in 100 mm-diameter Fisherbrand cell-culture plates (15–20 mL per plate). Lyophilized bacteria cultures were reconstituted and expanded according to instructions provided by the American Type Culture Collection (ATCC). To test the susceptibility, liquid cultures were grown for 18–24 h to an OD_{600} between 0.8 and 1 (corresponding to a viable count of approx. 10^7–10^8 CFU mL^{-1}). These cultures are referred to hereafter as "overnight cultures."

Susceptibility Testing: Active antibiotic release was quantified using a direct zone of inhibition assay based on the principle of the Kirby–Bauer susceptibility test;[40,41] the active antibiotic was quantified by comparing zones of clearance in bacterial lawns with the zones of clearance generated by standards of known antibiotic concentration. Samples (either silk biomaterials directly, sterile filter paper disks wetted with known volumes of a standard solution of known concentration or sterile filter paper disks wetted with known volumes of experimental solution of unknown concentration) were applied directly to agar plates coated with a mixture of dilute agar (half the recommended mass of powder per liter, or 20 g L^{-1}) and *S. aureus* overnight culture (5:1 volume:volume ratio), which grew to lawns overnight at 37 °C. After 24 h, the zone of inhibition was measured using Image J image-analysis software. The amount of drug released over 24 h was then determined by comparison of the sample zones of inhibition with the zones of inhibition of known standards on filter-paper disks. Extended release studies were carried out by transferring the test materials to new plates every 24 h.

Release Testing: In addition to quantifying rifampicin release from silk films and sponges using zone of clearance susceptibility testing, the rifampicin release was also determined by immersing drug-loaded silk materials in Dulbecco's PBS (0.5 mL) at 37 °C, removing and replacing the buffer at desired time points, and determining the amount of rifampicin released into the buffer using UV–vis spectroscopy at 475 nm.

In Vivo Testing: All of the animal studies were conducted under protocols reviewed and approved by the Tufts University Institutional Animal Care and Use Committee (IACUC). Male BALB/c mice weighing 20–25 g were shaved on the back and depilated with Nair (Carter–Wallace Inc., New York, NY). The mice were anesthetized with an intraperitoneal IP injection of ketamine/xylazine cocktail (90 mg kg^{-1} ketamine, 10 mg kg^{-1} xylazine) for surgery and infection. The operative area of skin was cleaned with alcohol, and subcutaneous injections containing live bacteria were given at four different sites on the shaved back of each animal. Each 100 µL injection contained 1×10^6 CFUs of *S. aureus*. After 24 h, raised bumps were observed at the four injection sites. Each animal (n = 5) received four treatments: one wound was untreated (control), one wound received an injection of ampicillin in sterile saline (100 µL, 250 µL mL^{-1}), one wound received an injection of unloaded silk hydrogel (4% (w/v), 100 µL) and one wound received an injection of silk hydrogel (4% (w/v)) loaded with ampicillin (100 µL, 250 µL mL^{-1}). The ampicillin concentration was selected based on the highest minimum inhibitory concentration (MIC) of ampicillin reported against clinical isolates of methicillin-resistant *S. aureus* (MRSA) (approx. 256 mg L^{-1}).[42,43] 24 h after treatment (48 h post-inoculation), the animals were anesthetized with an IP injection of a ketamine/xylazine cocktail (90 mg kg^{-1} ketamine, 10 mg kg^{-1} xylazine) and the infected tissue and surrounding tissues were excised and transferred to sterile 50 ml Falcon tubes containing sterile saline (10 mL). The animals were euthanized by carbon dioxide asphyxiation.

Excised tissue samples were homogenized using a T25 basic Ultra Turrax mechanical homeogenizer (IKA Works, Inc., Wilmington, NC). The numbers of bacteria in the homogenates were estimated by standard plate-count methods[44] using Tryptic Soy agar plates. Colonies were counted after 24 h of incubation at 37 °C. The bacterial count was expressed as the number of CFU per wound. To normalize for variability among the mice, CFU counts for each treatment modality were divided by the CFU count measured for the untreated wound and reported as a percentage.

Supporting Information

Supporting Information is available from the Wiley Online Library or from the author.

Acknowledgements

E.M.P. and T.V. carried out in vitro release testing, storage stability testing, and the majority of the writing. B.P. advised on the in vivo experimental design and performed all aspects of the in vivo studies involving animal handling. F.O. and D.L.K. oversaw all of the research and advised on experimental design and interpretation. This work was supported by the NIH (EB002520-05, EY020856, DE017207-01, EB003210) and AFOSR 9550-10-1-0172zsAJMn. The authors would like to thank Nikola Kojic and Reid McCabe for their assistance. The authors have no competing financial interests to declare.

Received: June 17, 2012
Published online: September 26, 2012

[1] R. Sauermann, R. Karch, H. Langenberger, J. Kettenbach, B. Mayer-Helm, M. Petsch, C. Wagner, T. Sautner, R. Gattringer, G. Karanikas, C. Joukhadar, *Antimicrob. Agents* **2005**, *49*, 4448.
[2] D. N. Gerding, A. J. Kozak, L. R. Peterson, W. H. Hall, *Antimicrob. Agents* **1980**, *17*, 1023.
[3] G. Han, L. R. Martinez, M. R. Mihu, A. J. Friedman, J. M. Friedman, J. D. Nosanchuk, *PLoS One* **2009**, *4*, e7804.
[4] S. K. Nandi, P. Mukherjee, S. Roy, B. Kundu, D. K. De, D. Basu, *Mater. Sci. Eng. C* **2009**, *29*, 2478.
[5] L. Englander, A. Friedman, *J. Clin. Aesthetic Dermatol.* **2010**, *3*, 45.
[6] J. S. Price, A. F. Tencer, D. M. Arm, G. A. Bohach, *J. Biomed. Mater. Res.* **1996**, *30*, 281.
[7] Z. Ruszczak, W. Friess, *Adv. Drug Delivery Rev.* **2003**, *55*, 1679.
[8] M. Zilberman, J. J. Elsner, *J. Controlled Release* **2008**, *130*, 202.
[9] D. Puppi, F. Chiellini, A. M. Piras, E. Chiellini, *Prog. Polym. Sci.* **2010**, *35*, 403.
[10] F. Siepmann, J. Siepmann, M. Walther, R. J. MacRae, R. Bodmeier, *J. Controlled Release* **2008**, *125*, 1.
[11] C. B. Abletshauser, R. Schneider, H. Rupprecht, *J. Controlled Release* **1993**, *21*, 149.
[12] A. Leal-Egaña, T. Scheibel, *Biotechnol. Appl. Biochem.* **2010**, *55*, 155.
[13] X. Tang, F. Ding, Y. Yang, N. Hu, X. Gi, *J. Biomed. Mater. Res. A* **2009**, *91A*, 166.

[14] L. Meinel, S. Hofmann, V. Karageorgiou, C. Kirker-Head, J. McCool, G. Gronowicz, L. Zichner, R. Langer, G. Vunjak-Novakovic, D. L. Kaplan, *Biomaterials* **2005**, *26*, 147.
[15] Y. K. Seo, H. H. Yoon, K. Y. Song, S. Y. Kwon, H. S. Lee, Y. S. Park, J. K. Park, *J. Orthop. Res.* **2009**, *27*, 495.
[16] B. Panilaitis, G. H. Altman, J. Chen, H. J. Jin, V. Karageorgiou, D. L. Kaplan, *Biomaterials* **2003**, *24*, 3079.
[17] G. H. Altman, F. Diaz, C. Jakuba, T. Calabro, R. L. Horan, J. Chen, H. Lu, J. Richmond, D. L. Kaplan, *Biomaterials* **2003**, *24*, 401.
[18] Y. Wang, D. D. Rudym, A. Walsh, L. Abrahamsen, H. J. Kim, H. S. Kim, C. Kirker-Head, D. L. Kaplan, *Biomaterials* **2008**, *29*, 3415.
[19] R. L. Horan, K. Antle, A. L. Collette, Y. Wang, J. Huang, J. E. Moreau, V. Volloch, D. L. Kaplan, G. H. Altman, *Biomaterials* **2005**, *26*, 3385.
[20] K. Numata, D. L. Kaplan, *Adv. Drug Delivery Rev.* **2010**, *62*, 1497.
[21] C. Vepari, D. L. Kaplan, *Prog. Polym. Sci.* **2007**, *32*, 991.
[22] B. D. Lawrence, M. Cronin-Golomb, I. Georgakoudi, D. L. Kaplan, F. G. Omenetto, *Biomacromolecules* **2008**, *9*, 1214.
[23] E. M. Pritchard, D. L. Kaplan, *Expert Opin. Drug Delivery* **2011**, *8*, 797.
[24] E. Wenk, H. P. Merkle, L. Meinel, *J. Controlled Release* **2011**, *150*, 128.
[25] S. Lu, X. Wang, Q. Lu, X. Hu, N. Uppal, F. G. Omenetto, D. L. Kaplan, *Biomacromolecules* **2009**, *10*, 1032.
[26] Q. Lu, X. Wang, X. Hu, P. Cebe, F. Omenetto, D. L. Kaplan, *Macromol. Biosci.* **2010**, *10*, 359.
[27] N. Guziewicz, A. Best, B. Perez-Ramirez, D. L. Kaplan, *Biomaterials* **2011**, *32*, 2642.
[28] S. Hofmann, C. T. Foo, F. Rossetti, M.Textor, G. Vunjak-Novakovic, D. L. Kaplan, H. P.Merkle, L. Meinel, *J. Controlled Release* **2006**, *111*, 219.
[29] X. Wang, X. Hu, A. Daley, O. Rabotyagova, P. Cebe, D. L. Kaplan, *J. Controlled Release* **2007**, *121*, 190.
[30] X. Wang, J. A. Kluge, G. G. Leisk, D. L. Kaplan, *Biomaterials* **2008**, *29*, 1054.
[31] X. Wang, E. Wenk, A. Matsumoto, L. Meinel, C. Li, D. L. Kaplan, *J. Controlled Release* **2007**, *117*, 360.
[32] M. Brisaert, M. Heylen, J. Plaizier-Vercammen, *Pharm. World Sci.* **1996**, *18*, 182.
[33] D.-H. Kim, J. Viventi, J. J. AmsJ. Xiao, L. Vigeland, Y.-S. Kim, J. A. Blanco, B. Panilaitis, E. S. Frechette, D. Contreras, D. L. Kaplan, F. G. Omenetto, Y. Huang, K.-C. Hwang, M. R. Zakin, B. Litt, J. A. Rogers, *Nature Mater.* **2010**, *9*, 511.
[34] W. Zhang, X. Wang, S. Wang, J. Zhao, L. Xu, C. Zhu, D. Zeng, J. Chen, Z. Zhang, D. L. Kaplan, X. Jiang, *Biomaterials* **2011**, *32*, 9415.
[35] Y. Wang, H.-J. Kim, G. Vunjak-Novakovic, D. L. Kaplan, *Biomaterials* **2006**, *2*, 6064.
[36] K. Tsioris, W. K. Raja, E. M. Pritchard, B. Panilaitis, D. L. Kaplan, F. G. Omenetto, *Adv. Mater.* **2012**, *22*, 330.
[37] S. Sofia, M. B. McCarthy, G. Gronowicz, D. L. Kaplan, *J. Biomed. Mater. Res.* **2001**, *54*, 139.
[38] U. J. Kim, J. Park, H. J. Kim, M. Wada, D. L. Kaplan, *Biomaterials* **2005**, *26*, 2775.
[39] A. Wilz, E. M. Pritchard, T. Li, J. Q. Lan, D. L. Kaplan, D. Boison, *Biomaterials* **2008**, *29*, 3609.
[40] A. W. Bauer, D. M. Perry, W. M. M. Kirby, *Arch. Intern. Med.* **1959**, *104*, 208.
[41] V. J. Boyle, M. E. Fancher, R. W. Ross, *Antimicrob. Agents Chemother.* **1973**, *3*, 418.
[42] Z. Q. Hu, W.-H. Zhao, Y. Hara, T. Shimamura, *J. Antimicrob. Chemother.* **2001**, *28*, 361.
[43] L. C. Braga, A. A. Leite, K. G. Xavier, J. A. Takahashi, M. P. Bemquerer, E. Chartone-Souza, A. M. Nascimento, *Can. J. Microbiol.* **2005**, *51*, 541.
[44] D. G. Saymen, P. Nathan, I. A. Holder, E. O. Hill, B. G. Macmillan, *Appl. Microbiol.* **1972**, *23*, 509.